Sala-Gascon, A.; Pérez-Botella, E.; Jorda Moret, JL.; Cantin Sanz, A.; Rey Garcia, F.; Valencia Valencia, S. (2021). ITQ-69: A Germanium-Containing Zeolite and its Synthesis, Structure Determination, and Adsorption Properties. Angewandte Chemie International Edition. 60(21):11745-11750. https://doi.org/10.1002/anie.202100822

COMMUNICATION

ITQ-69: A new Ge-containing zeolite and its synthesis, structure determination and adsorption properties

Andrés Sala,[a] Eduardo Pérez-Botella,[a] Jose L. Jordá,[a] Angel Cantín,[a] Fernando Rey*[a] and Susana Valencia*[a]

[a] Instituto de Tecnología Química
Universitat Politècnica de València - Consejo Superior de Investigaciones Científicas (UPV-CSIC)
Av. de los Naranjos, s/n, 46022, Valencia, Spain
E-mail: frey@itq.upv.es
E-mail: svalenci@itq.upv.es

Supporting information for this article is given via a link at the end of the document

Abstract: In this work, a new zeolite named as ITQ-69, has been synthesized, characterized and its application as selective adsorbent for industrially relevant light olefins/paraffins separations has been assessed. This material has been obtained as pure germania as well as silica-germania zeolites with different Si/Ge ratios using a diquaternary ammonium cation as organic structure directing agent. Its structure was determined by single-crystal X-Ray diffraction showing a triclinic unit cell forming a tridirectional small pore channel system (8 × 8 × 8R). Also, it has been found that Si preferentially occupies some special T sites of the structure as deduced from Rietveld analysis of the powder X-ray diffraction patterns. In addition, the new zeolite ITQ-69 has been found to be stable upon calcination and thus, its adsorption properties were evaluated, showing a promising kinetic selectivity for light olefin separations in the C3 fraction.

Zeolites are inorganic microporous materials that present a well-defined crystalline structure comprising channel systems with pore apertures of molecular dimensions. These porous materials are widely used in ion-exchange, catalysis and adsorption and separation processes.[1–3] The broad range of zeolite applications is a consequence of their specific chemical composition and unique porous structures.

Therefore, the search and development of new zeolites are among the main targets in the field of zeolite science since the pioneering work reported by Barrer in the 1940s.[4] The most fruitful strategies for discovering new zeolites rely on the use of specially designed organic structure directing agents (OSDAs),[5] as well as heteroatom substitution in the zeolite structure.[6,7] On this regard, the incorporation of germanium as heteroatom emerges as an excellent approach towards obtaining new zeolites.[8–10] Up to now, more than fifty different germanium containing zeolitic structures have been described since the 70s.[11,12]

The larger germanium atomic radius introduces framework flexibility and high tolerance in the crystal structure to acute T-O-T bond angles.[13–15] Thus, very often the incorporation of germanium directs towards zeolites containing double four ring cages (D4R) due to its preferential occupation of those sites.[8,16–23] The presence of small cages, such as D4R, results in microporous solids of very low framework densities as predicted by Meier.[24] Theoretical calculations have confirmed this interpretation, and support the preferential occupation of Ge atoms in D4R cages in silicagermania zeolites.[22,25]

The discovery of new zeolitic materials with varied structures opens the possibility of selecting the most appropriated material for a given separation of interest. Thus, structural elucidation is one of the mandatory steps in designing selective zeolite adsorbents. Differently than silica based zeolites, pure germania and silica-germania zeolites very often grow forming very large crystals, allowing their structural elucidation by single-crystal X-ray diffraction (SCXRD) methods.[21,26–29] Thus, solving their structures does not require the use of more complex approaches such as electron diffraction (ED) or high-resolution transmission electron microscopy (HRTEM) imaging, combined with high resolution powder diffraction techniques (HRPXRD).[30–32]

Furthermore, several germanosilicates have demonstrated excellent performance in applications of high industrial interest.[8,19] For instance, some Ge-containing zeolites show unique catalytic properties or promising perspectives for separation processes even of racemic mixtures .[15,20,33]

In this way, we have focused our interest on an industrially very relevant process, which is light olefins/paraffins separations. Light olefins are mostly produced by thermal or catalytic cracking of hydrocarbons and their separation is currently done by cryogenic distillation, this being one of the most energy demanding processes in refineries.[34] Thus, developing these separations at near ambient temperature is a matter of academic and industrial interest.[35–41]

This communication describe the synthesis, structural elucidation and application for short olefins/paraffins separations of a new zeolite, ITQ-69, using the organic dication 2,5,5,3a,3b-tetramethyloctahydropyrrolo[3,4]pyrrole-2,5-diium (R) as organic structure directing agent (OSDA). Details of OSDA preparation and synthesis of zeolite ITQ-69 with different Si/Ge ratios are given as Supporting Information.

Zeolite ITQ-69 was obtained either in fluoride or hydroxide media in the synthesis gel compositions comprised between the pure germania and Si/Ge=5. For lower Ge contents, ITQ-69 crystallized with BEC and AST in different proportions in fluoride media, whilst amorphous solids are obtained in alkaline syntheses, as reported in Tables S1 and S2.

It is observed that high Ge content favors the crystallization of zeolite ITQ-69 as pure phase and zeolite BEC appears when the Si/Ge increases above 1. Also, it is notorious that zeolites BEC and ITQ-69 are formed in crystallization gels of Si/Ge = 1, but as the crystallization time increases zeolite BEC disappears in the final solid and the product yield decreases, suggesting that zeolite BEC is dissolved as crystallization time increases. Finally, it is worth to mention that, when synthesized in alkaline media, zeolite ITQ-69 is formed in a wide range of gel composition and crystallization times as a pure phase. This finding may be related to the presence of disconnected T atoms it the structure ITQ-69 as discussed below.

The characterization of zeolites ITQ-69 was done on the selected as-made samples listed in Table S3. The chemical analyses of the samples clearly evidence that there is a preferential incorporation of germanium respect to silicon in the solids, as deduced from lower Si/Ge ratios of the zeolites compared to the synthesis gels.

The powder X-Ray diffraction (XRD) patterns of the selected zeolites ITQ-69 are given in Figure 1. There, it is clearly evidenced that Ge-richer samples show significantly better peak resolution than those of lower Ge content.

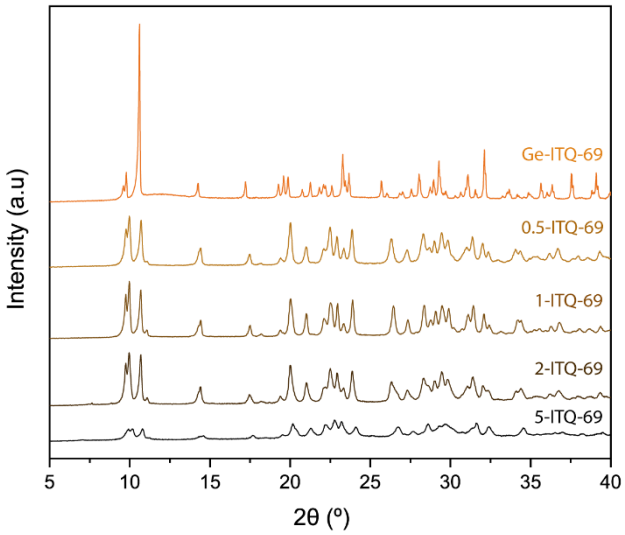

Figure 1. PXRD patterns of the as-made ITQ-69 zeolites in the with different Si/Ge ratios.

Interestingly, the presence of HF in the synthesis gel leads to the formation of zeolite ITQ-69 but, surprisingly, fluoride is not incorporated in the structure, as it was confirmed by ^{19}F MAS NMR spectroscopy (not shown).

The integrity of the OSDA inside the zeolite was confirmed by elemental analysis (EA) and solid-state ^{13}C-NMR studies. EA reveals a C/N molar ratio very close to 5.0 in the as-prepared zeolite, which matches the theoretical value of 5 for the pure OSDA (Table S3). The ^{13}C-NMR spectrum of the as-made ITQ-69 material shows signals at 39.8, 51.2, 52.8, 68.4 ppm that correspond to those of the pure organic cation, confirming that it remains intact inside the zeolite pores (Figure S1). Furthermore, thermogravimetric analysis (TGA) shows that the main weight loss of 17.5 % occurs between 673 and 1000 K (Figure S2). This is attributed to the combustion of the occluded organic incorporated in ITQ-69, suggesting a significant fraction of microporosity in the material.

The as-made 1-ITQ-69 sample (Si/Ge=0.7) was calcined under dry air using an 'in-situ' chamber attached to the XRD instrument avoiding the contact of the sample with the atmospheric moisture. The as-made and calcined XRD patterns are compared in Figure S3, there it can be seen that the structural integrity is mostly retained upon calcination at 823 K, although a clear structural distortion occurs as indicated by the broadening of some X-ray diffraction peaks.

By using a similar calcination procedure, the isotherms of N_2 at 77 K and Ar at 87 K of the calcined ITQ-69 were measured. The N_2 and Ar isotherms are shown in Figures S4 and S5, respectively. Both fit type I isotherms, confirming the microporous nature of zeolite ITQ-69.

The Brunauer-Emmet-Teller (BET) surface area and t-plot micropore volume were calculated from the N_2 adsorption isotherm (Figure S4) and resulted to be 248 m^2g^{-1} and 0.093 $cm^3 g^{-1}$, respectively. It has to be noted that the analyzed sample contains a large amount of Ge, thus for the sake of comparison, it is worth referring these values to the hypothetical pure silica ITQ-69 material. When this is done, the recalculated surface area and micropore volume for the pure silica material become 356 m^2g^{-1} and 0.13 cm^3g^{-1}, respectively. These values are compatible with small pore zeolites having multidimensional channel systems. Additionally, the pore size distribution analysis obtained by applying the Horvath-Kawazoe formalism to the Ar isotherm revealed that ITQ-69 possesses narrowly distributed micropores with apertures centered at around 5 Å which is typically observed in many 8R zeolites (Figure S5).

The size and morphology of ITQ-69 crystals were examined by Field Emission-Scanning Electron Microscopy (FE-SEM). The micrographs showed the presence of very large crystals, especially in the case of the Ge-richest samples (Figure S6). In the case of the pure germania ITQ-69 zeolite, crystals of several tenths of microns were observed. This allowed the acquisition of single-crystal X-ray diffraction (SCXRD) data on a selected single crystal specimen of zeolite ITQ-69 (crystal dimensions: 70 × 40 × 20 μm^3). The SCXRD measurement was performed at 225 K. Data analysis can be downloaded from The Cambridge Structural Database as CSD-2056162 and reveal that as-made ITQ-69 crystallizes in a triclinic system, with space group P-1. The calculated cell parameters were a = 9.2252(2) Å, b = 9.2383(2) Å, c = 9.9724(2) Å, α = 87.159(1)°, β = 65.126(1)°, γ = 88.309(1)°, and V = 770.08(3) $Å^3$ (Table S4). The analysis of the SCXRD data allowed determining the location of all the framework atoms, as well as those corresponding to the occluded OSDA (Further details on data acquisition and analysis are given in Structure Determination section in the Supporting Information).

The structure of ITQ-69 can be described starting from a basic cage [4^2 5^4 6^2] (Figure 2A). It is remarkable the presence of the unconnected T1 atoms, which appear as a pair of well-defined T1-OH groups pointing to the inner of the cage. The subsequent [4^2 5^4 6^2] cages fuse to each other by sharing the T6-O12-T6 edge, forming chains along the a axis (Figure 2B). It must be noted that,

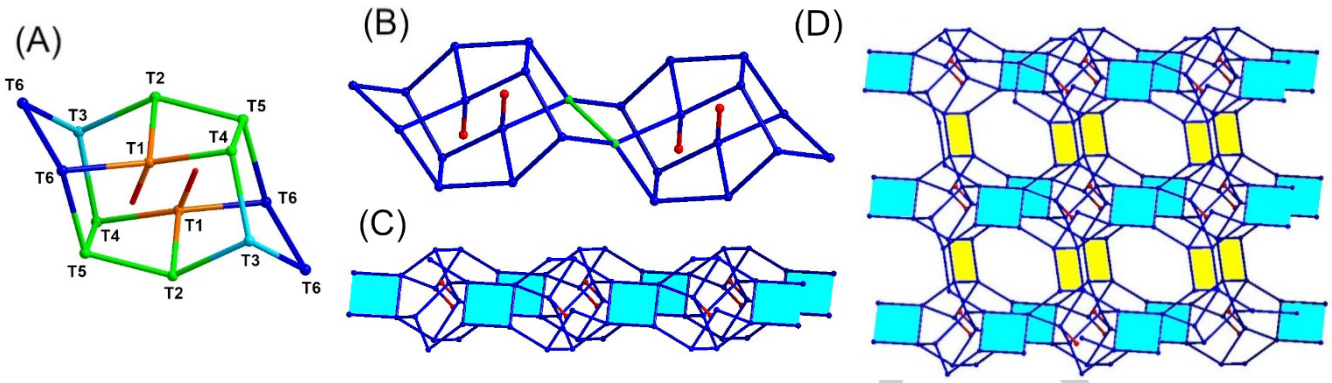

Figure 2. Description of the construction of the structure of ITQ-69 (A) basic cage [4^2 5^4 6^2] and its different T-sites (red: -OH groups); (B) chains along the *a* axis (sharing edge in green); (C) connections of chains through 4R (in light blue) in the *c* direction, forming layers in the *ac* plane; (D) connections of layers through 4R (in yellow) in the *b* direction, forming the complete tridimensional structure. OSDA and oxygen atoms (except O1, corresponding to the -OH groups) have been removed for clarity.

due to geometrical and symmetry restrictions, the T6-O12-T6 average angle appears to be 180˚, indicating a certain mobility or disorder of the O12 atoms around that position to give more physically feasible real angles. Then, these chains connect to their parallel neighbors through 4R units, involving the T3 and T4 atoms, in the *c* direction, forming layers in the *ac* plane (Figure 2C). Finally, the layers stack and connect to their neighbors forming 4R units along *b*, which involve the connections of the T2 and T5 sites, resulting in the final tridimensional structure (Figure 2D). Despite the presence of fluoride anions and germanium in the synthesis gel, both claimed as strong inorganic structure directing agents towards D4R containing frameworks,[13] zeolite ITQ-69 presents single 4R units but not D4R.

This structure presents a tridirectional system of interconnected straight small pore channels (8 × 8 × 8R) with elliptical apertures (5.4 × 3.1 Å, 5.7 × 2.7 Å and 6.1 × 2.1 Å along *a*, *b* and *c*, respectively). Finally, the OSDA molecules are located at the channel intersections. The projections of the ITQ-69 structure along the main crystallographic axes are shown in Figures S7.

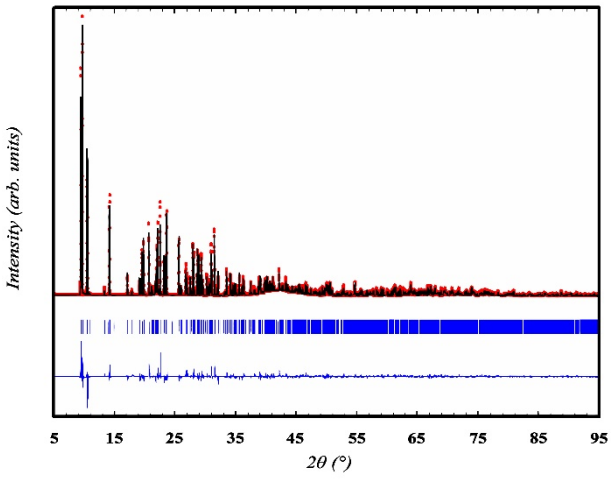

Figure 3. Rietveld refinement of the powder X-ray diffraction patter of as-made pure germania ITQ-69. Red data points show the observed XRPD pattern; black line along these points is the calculated XRPD pattern; blue line is the difference profile. The blue vertical tick marks below the pattern give the positions of the Bragg reflections. Residual values: Rwp = 0.18, Rexp =0.03, RB = 0.11, RF = 0.09. Wavelength corre-sponding to CuKα1.

In a subsequent step, the powder X-ray diffraction (PXRD) pattern of the as-made pure germania sample was measured at room temperature and refined using the Rietveld method (Figure 3).[42] The objective of this step was ensuring that the measured single crystal was representative of the whole sample, confirming that no appreciable impurities were present in the material, and determining the structure at room temperature. So, the refinement confirmed that, effectively, the as-made sample was a pure material, and no significant changes occur in that range of temperatures in the cell parameters or the framework structure.

The Rietveld analysis of the PXRD data corresponding to samples obtained with different Si/Ge ratios gave similar results, with small variations of the unit cell parameters. As expected, a reduction of the unit cell volume is observed when replacing Ge with Si from pure Ge (V= 770.58(1) Å^3) to a ratio of Si/Ge= 0.4 (745.19(6) Å^3), Si/Ge= 0.7 (738,69(6) Å^3) and Si/Ge= 1.2 (737,9(2) Å^3), due to the smaller atomic radius of Si compared with Ge. (Table S5)

In addition, it has been possible to determine the preferential location of Si and Ge atoms in the different T-sites of the silicogermanate forms of the as made zeolites ITQ-69 with Si/Ge ratios 0.4, 0.7 and 1.2. The refined data indicate that, as observed in several other zeolitic silicogermanates (Table S6 and Figure S8), preferential occupation of certain sites with Si exists, whilst Ge preferentially occupies other T sites. In this sense, the preferred T-site for Si atoms corresponds to the positions T6 and T3, the only T-site that does not form 4R or T-OH groups. The T1 position is occupied preferentially by Ge atoms, where the unconnected T atoms are located (Figure 2A), yielding germanol groups (Ge-OH). On the other hand, a less evident preferential occupation is found for T5, T4 and T2. The presence of Ge-OH groups is further supported by the presence of its characteristic band at 3677 cm^{-1} that has been observed in other Ge-containing zeolites, being more intense than that appearing at 3744 cm^{-1} assigned to Si-OH groups. Also, two broad and weak bands at ~ 3645 and 3450 cm^{-1} appear, suggesting the presence of a minor amount of bridged T-OH groups (T: Si or Ge) (Figure S9). [43–46]

Some small pore zeolites have been found to be promising adsorbents for selective separations of small molecules, such as CO_2/CH_4, ethylene/ethane, propylene/propane or linear butenes/butane.[32,37,47–51] Here, we have evaluated the adsorption properties of zeolite ITQ-69 for separating propylene and

butylenes from the C3 and C4 hydrocarbon distillation fractions, respectively.

The adsorption isotherms and kinetics of propane, propylene, butane, 1-butene, cis-2-butene and trans-2-butene on the 2-ITQ-69 sample (Si/Ge=1.2) were measured (further are given in Adsorption Experiments section in the Supporting Information). The propylene and propane isotherms are shown in Figure S10. There, it can be observed that propane uptake of zeolite ITQ-69 increases with adsorption temperature, indicating that propane does not reach thermodynamic equilibrium under the experimental conditions used in this work. This clearly demonstrates that there are severe diffusional restrictions for propane adsorption in zeolite ITQ-69. Conversely, propylene reaches equilibrium at any pressure and/or temperature. The adsorption data of propylene can be fitted using the Dual Site

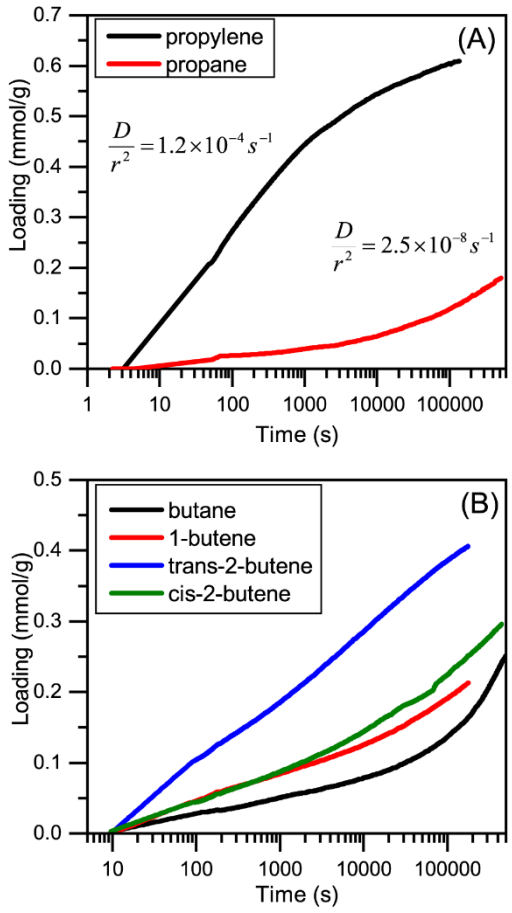

Figure 5. Adsorption kinetics at 298 K and 30 kPa of C3 (A) and C4 (B) olefins and paraffins on 2-ITQ-69 sample (Si/Ge = 1.2). Note that for calculating the propane D/r^2 the same maximum uptake as for propylene was assumed.

Langmuir (DSL) model (Table S7). The calculated isosteric heat of adsorption at any experimental coverage of propylene is 23 ± 2 kJ/mol, very close to that found in other small pore pure silica zeolites, such as DD3R and ITQ-32.[37,52] These results encouraged us to perform a more detailed study on the adsorption kinetics of C3 and C4 linear hydrocarbons. The propane and propylene uptakes versus time are plotted in Figure 5A. These results clearly show that propylene diffuses much faster than propane through the microporous system of zeolite ITQ-69, suggesting that both hydrocarbons can be kinetically separated using this new zeolite as a selective adsorbent. The kinetic plots were fitted using the Crank solution to the equation of diffusion in spherical particles[53,54] and the diffusion time constants (D/r^2, where D is the Fickian diffusion coefficient and r is the averaged radius) were calculated and included in Figure 5A. The $D_{C3^=}$ / D_{C3} ratio was of an order of 10^4, indicating that zeolite ITQ-69 is an excellent adsorbent for the kinetic separation of propylene and propane. These values are comparable to other zeolites, such as ITQ-32 and DD3R, in both kinetic selectivity and propylene uptake (when recalculated as mmol/g_{SiO2}) (Table S8).[37,52,55]

Furthermore, zeolite ITQ-69 was studied for separation of linear butenes from butane. The adsorption kinetics are shown in Figure 5B. There, it can be seen that trans-2-butene is adsorbed much faster than other C4 hydrocarbons. However, the overall adsorption rates of the C4 fraction are too low for applying any model that permits us to calculate reliable numerical values on diffusion. In these experiments, the hydrocarbon loadings were very far from reaching thermodynamical equilibrium and thus, the maximum adsorption uptake cannot be obtained for any of the C4 hydrocarbons. Structural damage of zeolite was discarded since CO_2 adsorption isotherms on the fresh calcined sample and that one after hydrocarbon adsorption experiments were coincident (Figure S11).

This slow kinetics of adsorption of trans-2-butene hinders the potential application of zeolite ITQ-69 for C4 separation in swing adsorption processes but, if achieved, ITQ-69 prepared as a membrane may potentially separate this fraction.

In summary, a new zeolite named as ITQ-69 has been synthetized and its structure has been determined. The structural topology of this zeolite presents a tridirectional small pore channel system, which is specially appropriated for propylene/propane kinetic separation. Thus, zeolite ITQ-69 may be a promising adsorbent for selective propylene recovery from the C3 fraction in refineries.

Acknowledgements

The authors acknowledge the Spanish Ministry of Science, Innovation and Universities (MCIU) for their funding via project RTI2018-101784-B-I00 and Program Severo Ochoa SEV-2016-0683. AS and EPB thanks for their grants BES-2016-078684 and FPU15/01602, respectively. The Microscopy Service of the UPV is acknowledged for their help in sample characterization. By last, authors would like to thank the use of RIAIDT-USC analytical facilities, especially to Dr. Antonio L. Llamas for extremely useful comments on SCXRD analyses.

Keywords: zeolite • structural elucidation • adsorption properties • propylene separation

[1] J. Cejka, A. Corma, S. Zones, *Zeolites and Catalysis: Synthesis, Reactions and Applications*, John Wiley & Sons, **2010**.
[2] J. Jiang, J. Yu, A. Corma, *Angew. Chemie Int. Ed.* **2010**, *49*, 3120–3145.
[3] E. Pérez-Botella, M. Palomino, S. Valencia, F. Rey, in *Nanoporous Mater. Gas Storage*, Springer, **2019**, pp. 173–208.
[4] R. M. Barrer, *J. Chem. Soc.* **1948**, 127–132.
[5] M. Moliner, F. Rey, A. Corma, *Angew. Chemie - Int. Ed.* **2013**, *52*, 13880–13889.
[6] S. I. Zones, *Microporous Mesoporous Mater.* **2011**, *144*, 1–8.
[7] J. Li, A. Corma, J. Yu, *Chem. Soc. Rev.* **2015**, *44*, 7112–7127.

[8] A. Corma, M. J. Diaz-Cabañas, J. Martínez-Triguero, F. Rey, J. Rius, *Nature* **2002**, *418*, 514–517.
[9] Y. Luo, S. Smeets, Z. Wang, J. Sun, W. Yang, *Chem. - A Eur. J.* **2019**, *25*, 2184–2188.
[10] L. Bieseki, R. Simancas, J. L. Jordá, P. J. Bereciartua, Á. Cantín, J. Simancas, S. B. Pergher, S. Valencia, F. Rey, A. Corma, *Chem. Commun.* **2018**, *54*, 2122–2125.
[11] L. Lerot, G. Poncelet, J. J. Fripiat, *Mater. Res. Bull.* **1974**, *9*, 979–987.
[12] C. Baerlocher, L. B. McKusker, "Database of zeolite structures," can be found under http://www.iza-structure.org/databases/ **2020.**
[13] M. Opanasenko, M. Shamzhy, Y. Wang, W. Yan, P. Nachtigall, J. Čejka, *Angew. Chemie - Int. Ed.* **2020**, *59*, 19380–19389.
[14] Y. Li, J. Yu, *Chem. Rev.* **2014**, *114*, 7268–7316.
[15] J. J. Gutiérrez-Sevillano, S. Calero, S. Hamad, R. Grau-Crespo, F. Rey, S. Valencia, M. Palomino, S. R. G. Balestra, A. R. Ruiz-Salvador, *Chem. - A Eur. J.* **2016**, *22*, 10036–10043.
[16] B. W. Boal, M. W. Deem, D. Xie, J. H. Kang, M. E. Davis, S. I. Zones, *Chem. Mater.* **2016**, *28*, 2158–2164.
[17] A. Corma, M. J. Díaz-Cabañas, F. Rey, S. Nicolopoulus, K. Boulahya, *Chem. Commun.* **2004**, *4*, 1356–1357.
[18] J. L. Paillaud, B. Harbuzaru, J. Patarin, N. Bats, *Science* **2004**, *304*, 990–992.
[19] M. Moliner, M. J. Díaz-Cabañas, V. Fornés, C. Martínez, A. Corma, *J. Catal.* **2008**, *254*, 101–109.
[20] J. Sun, C. Bonneau, Á. Cantín, A. Corma, M. J. Díaz-Cabãas, M. Moliner, D. Zhang, M. Li, X. Zou, *Nature* **2009**, *458*, 1154–1157.
[21] A. Corma, M. J. Díaz-Cabañas, J. Jiang, M. Afeworki, D. L. Dorset, S. L. Soled, K. G. Strohmaier, *Proc. Natl. Acad. Sci.* **2010**, *107*, 13997–14002.
[22] A. Corma, M. T. Navarro, F. Rey, J. Rius, S. Valencia, *Angew. Chemie - Int. Ed.* **2001**, *40*, 2277–2280.
[23] A. Corma, F. Rey, S. Valencia, J. L. Jordá, J. Rius, *Nat. Mater.* **2003**, *2*, 493–497.
[24] G. O. Bnmner, W. M. Meier, *Nature* **1989**, *337*, 146–147.
[25] T. Blasco, A. Corma, M. J. Díaz-Cabañas, F. Rey, J. A. Vidal-Moya, C. M. Zicovich-Wilson, *J. Phys. Chem. B* **2002**, *106*, 2634–2642.
[26] T. Conradsson, M. S. Dadachov, X. D. Zou, *Microporous Mesoporous Mater.* **2000**, *41*, 183–191.
[27] H. Li, M. Eddaoudi, D. A. Richardson, O. M. Yaghi, *J. Am. Chem. Soc.* **1998**, *120*, 8567–8568.
[28] Z. B. Yu, Y. Han, L. Zhao, S. Huang, Q. Y. Zheng, S. Lin, A. Córdova, X. Zou, J. Sun, *Chem. Mater.* **2012**, *24*, 3701–3706.
[29] L. Tang, L. Shi, C. Bonneau, J. Sun, H. Yue, A. Ojuva, B.-L. Lee, M. Kritikos, R. G. Bell, Z. Bacsik, J. Mink, X. Zou, *Nat. Mater.* **2008**, *7*, 381–385.
[30] T. Willhammar, Y. Yun, X. Zou, *Adv. Funct. Mater.* **2014**, *24*, 182–199.
[31] F. Gramm, C. Baerlocher, L. B. McCusker, S. J. Warrender, P. A. Wright, B. Han, S. B. Hong, Z. Liu, T. Ohsuna, O. Terasaki, *Nature* **2006**, *444*, 79–81.
[32] P. J. Bereciartua, Á. Cantín, A. Corma, J. L. Jordá, M. Palomino, F. Rey, S. Valencia, E. W. Corcoran, P. Kortunov, P. I. Ravikovitch, *Science* **2017**, *358*, 1068–1071.
[33] S. K. Brand, J. E. Schmidt, M. W. Deem, F. Daeyaert, Y. Ma, O. Terasaki, M. Orazov, M. E. Davis, *Proc. Natl. Acad. Sci. U. S. A.* **2017**, *114*, 5101–5106.
[34] D. S. Sholl, R. P. Lively, *Nature* **2016**, *532*, 435–437.
[35] H. Järvelin, J. R. Fair, *Ind. Eng. Chem. Res.* **1993**, *32*, 2201–2207.
[36] J. J. Gutiérrez-Sevillano, D. Dubbeldam, F. Rey, S. Valencia, M. Palomino, A. Martín-Calvo, S. Calero, *J. Phys. Chem. C* **2010**, *114*, 14907–14914.
[37] M. Palomino, A. Cantín, A. Corma, S. Leiva, F. Rey, S. Valencia, *Chem. Commun.* **2007**, *24*, 1233–1235.
[38] J. Gascon, W. Blom, A. van Miltenburg, A. Ferreira, R. Berger, F. Kapteijn, *Microporous Mesoporous Mater.* **2008**, *115*, 585–593.
[39] J. G. Min, K. C. Kemp, S. B. Hong, *Microporous Mesoporous Mater.* **2020**, *294*, 109833.
[40] J. Gi, K. C. Kemp, K. S. Kencana, R. R. Mukti, S. Bong, *Chem. Eng. J.* **2020**, 127422.
[41] D. H. Olson, M. A. Camblor, L. A. Villaescusa, G. H. Kuehl, *Microporous Mesoporous Mater.* **2004**, *67*, 27–33.
[42] J. Rodriguez-Carvajal, *FullProf*, France, **2001**.
[43] H. Kosslick, V. A. Tuan, R. Fricke, C. Peuker, *Berichte der Bunsengesellschaft für Phys. Chemie* **1992**, *96*, 1761–1765.
[44] L. G. A. Van de Water, J. C. Van der Waal, J. C. Jansen, M. Cadoni, L. Marchese, T. Maschmeyer, *J. Phys. Chem. B* **2003**, *107*, 10423–10430.
[45] S. Leiva, M. J. Sabater, S. Valencia, G. Sastre, V. Fornés, F. Rey, A. Corma, *Comptes Rendus Chim.* **2005**, *8*, 369–378.
[46] N. Kasian, T. I. Koranyi, G. Vanbutsele, K. Houthoofd, J. A. Martens, C. E. A. Kirschhock, *Top. Catal.* **2010**, *53*, 1374–1380.
[47] D. M. Ruthven, *Chemie-Ingenieur-Technik* **2011**, *83*, 44–52.
[48] M. Palomino, A. Corma, J. L. Jordà, F. Rey, S. Valencia, *Chem. Commun.* **2012**, *48*, 215–217.
[49] M. Palomino, A. Corma, F. Rey, S. Valencia, *Langmuir* **2010**, *26*, 1910–1917.
[50] T. D. Pham, R. F. Lobo, *Microporous Mesoporous Mater.* **2016**, *236*, 100–108.
[51] J. G. Min, K. C. Kemp, S. B. Hong, *J. Phys. Chem. C* **2017**, *121*, 3404–3409.
[52] H. Abdi, H. Maghsoudi, *Microporous Mesoporous Mater.* **2020**, *307*, 110513.
[53] J. Crank, *The Mathematics of Diffusion*, **1975**.
[54] J. Karger, D. M. Ruthven, *Diffusion in Zeolites and Other Microporous Solids*, John Wiley & Sons, Inc., New York, **1992**.
[55] W. Zhu, F. Kapteijn, J. A. Moulijn, M. C. Den Exter, J. C. Jansen, *Langmuir* **2000**, *16*, 3322–3329.

Entry for the Table of Contents

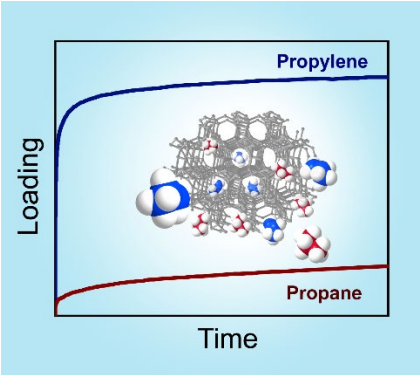

ITQ-69 has been synthesized, characterized and its application as selective adsorbent for light olefins/paraffins has been tested.

@ITQ_UPVCSIC